Research Report

98-13

Dual Stator Winding Induction Machine Drive

A. Munoz-Garcia, T.A. Lipo

Wisconsin Power Electronic Research Center
University of Wisconsin-Madison
Madison WI 53706-1691

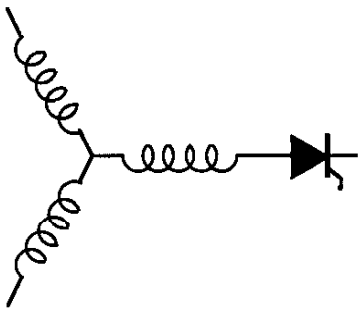

Wisconsin
Electric
Machines &
Power
Electronics
Consortium

University of Wisconsin-Madison
College of Engineering
Wisconsin Power Electronics Research Center
2559D Engineering Hall
1415 Engineering Drive
Madison WI 53706-1691

DUAL STATOR WINDING INDUCTION MACHINE DRIVE

Alfredo Muñoz-García Thomas A. Lipo
Department of Electrical and Computer Engineering
University of Wisconsin – Madison
1415 Engineering Drive
Madison, WI 53706-1691 USA
Tel.: (608) 262-0727 Fax: (608) 262-1267 email: alfredo@cae.wisc.edu - lipo@engr.wisc.edu

Abstract— **A new dual stator winding induction machine drive is described in this paper. The new machine consists of a squirrel cage induction motor having two stator windings wound for 2 and 6 poles which are simultaneously fed from two independent variable frequency power supplies. The proposed drive offers the advantage of simultaneously producing two independent electromagnetic torques which can be controlled to produce any desired combination of output torque. Since each torque component is controlled by an independent set of stator currents a minimum operating frequency can be set for each stator winding and still achieve exactly zero or near zero speed and rated torque operation. This feature is specially important to minimize the negative impact of the stator resistance influence at low speed operation. The drive is well suited for either constant volts per Hz (V/f) or field oriented (FO) operation.**

The occurrence of circulating harmonic currents, common to traditional dual stator machines, is completely eliminated by the dissimilar pole number in each stator winding.

I. Introduction

The use of a common magnetic structure shared by two sets of stator windings was first introduced in the late 1920's as a means to increase the power capability of large synchronous generators [1]. Since then, dual stator machines have been used in many other applications, ranging from synchronous machines with AC and DC outputs [2] and as current source inverters [3] to large pumps, compressors and rolling mills driven by induction motors, to name a few. They have also been used to improve the reliability at the system level [4], [5].

Dual stator machines are normally constructed by "splitting" the stator winding into two displaced but identical windings [6]. However, this results in mutual coupling between the stators, causing circulating harmonic currents [7] as well as coupling between the electromagnetic torques produced by each stator winding [8]. This means of splitting the winding is a major drawback because the circulating currents add extra stator losses and demand larger semiconductor device ratings.

The dual stator winding induction machine proposed in this paper differs from the "standard" dual stator machine in that the two stator windings are wound for a dissimilar number of poles. This approach, in principle, eliminates the net magnetic coupling between the stator windings and decouples the torques produced by each set of stator currents. Also, circulating harmonic currents, due to the so-called mutual leakage coupling, are completely eliminated. Since the output torque corresponds to the algebraic sum of two independent torques, the stator frequency is no longer determined uniquely by the rotor speed and the slip frequency but also by the added variable of a second torque component. From the perspective of control theory this adds one degree of freedom to the system.

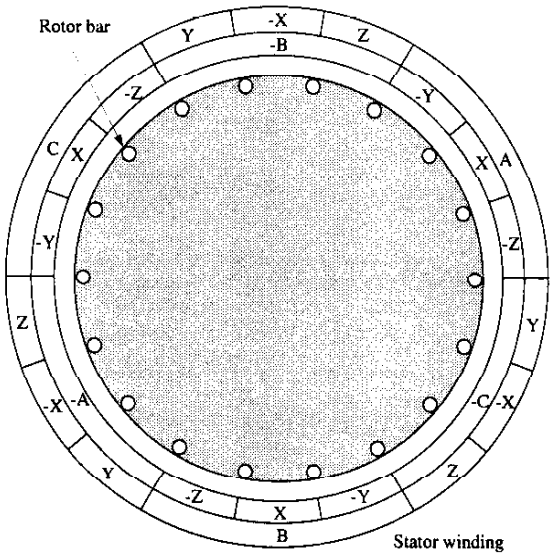

Fig. 1. Dual stator winding distributions.

Additionally, by having two independent torque components the low frequency operation, including stand still, can be improved. This is particularly important for constant volts per hertz operation at zero speed, where the influence of the stator resistance becomes dominant. In the proposed machine zero speed operation does not translate into zero excitation frequency, hence significantly reducing the influence of the Ir voltage drop.

II. Dual Stator Winding IM Drive

The stator of the proposed machine is constructed by dividing the original three phase winding into two separate three phase windings wound for a dissimilar number of poles. Any combination of dissimilar pole number could be used, however, to better utilize the magnetic material, avoid localized saturation and additional stator losses, it is found that the most advantageous configuration is a 2-6 pole combination. Such an arrangement is shown in Fig. 1. From the perspective of magnetic material utilization it is convenient to choose a pole number combination that, in

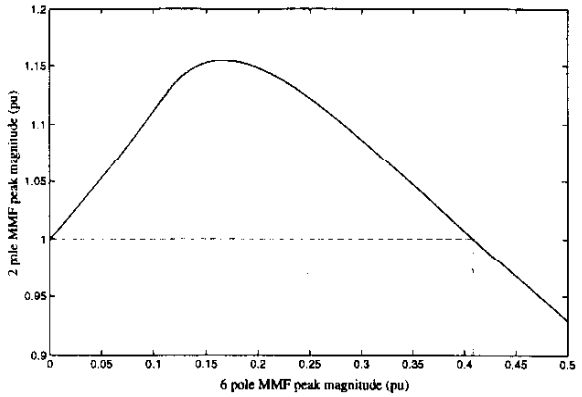

Fig. 2. 6 pole peak MMF for constant total peak MMF.

the steady state, will tend to produce a nearly trapezoidal MMF distribution. This type of distribution is most efficiently obtained by choosing the number of poles in the ratio 1:3. On the other hand, the magnetizing inductance varies inversely proportional to the square of the number of poles, hence a machine with a large number of poles results in low power factor and reduced efficiency. In addition, to achieve a sinusoidal winding distribution the stator winding must be distributed among several slots, therefore, for a given stator inner diameter, the number of slots per pole decreases in proportion to the number of poles. Also, for a given rotor speed, the stator frequency increases directly proportional to the number of poles. This translates into additional losses, in the machine and in the power converter, further reducing the efficiency. All these factors suggest that the maximum number of poles should be kept to a minimum, hence the best combination is to choose 2 and 6 poles.

The total MMF distribution in the airgap corresponds to the sum of the MMF's produced by each stator winding. To avoid the presence of highly saturated points and, at the same time, fully utilize the magnetic core it is desirable to maintain the total peak flux density distribution equal to that created by a two pole winding acting alone.

Figure 2 shows the peak magnitude of the 2 pole MMF, as a function of the 6 pole peak MMF, for a constant total peak MMF. The optimum distribution corresponds to choosing a 6 pole MMF equal to approximately 40% that of the 2 pole distribution. In this case the total MMF and the 2 pole MMF have the same peak amplitude, thus preserving the saturation level.

The rotor of the proposed machine corresponds to that of a standard squirrel cage type. This construction guarantees that both stator current distributions will simultaneously couple with the rotor flux to produce the desired torque.

Because of the decoupling effect produced by the difference in pole number, the proposed dual stator machine behaves as two independent induction machines that are mechanically coupled through the shaft. Therefore, all the known control techniques used in induction machine drives are also applicable to the dual stator winding machine. This includes both scalar constant volts per hertz

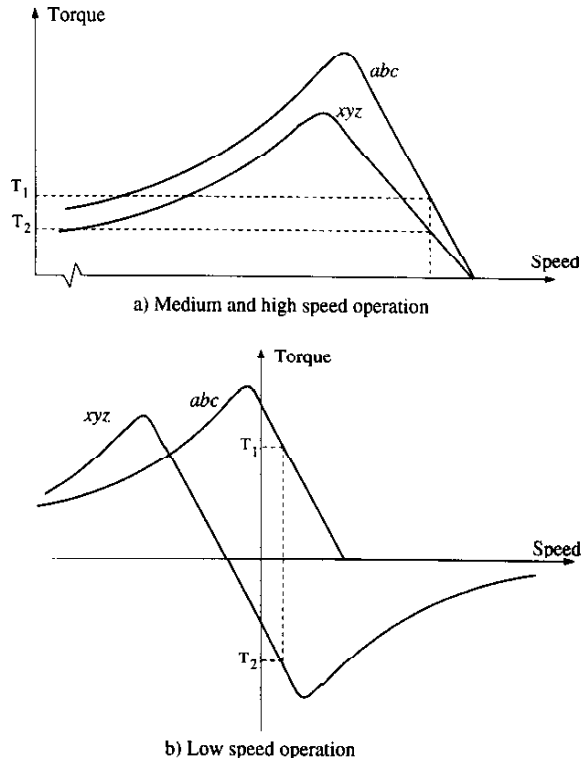

Fig. 3. General control strategy.

(V/f) as well as vector control or field orientation (FO). The basic control method is to generate two torque commands such that combined they produce the required output torque. By choosing adequate current commands the two individual torques can be added or subtracted, hence providing an extra handle to control the excitation frequency. Two distinct modes of operation are considered: low speed where the two torques are subtracted and medium to high speed, where the torques are added. This is shown in Fig. 3.

A further discussion of the control method will be delayed until after a derivation of the machine model is conducted and it will be presented in IV.

III. Machine Model

Given the particular characteristics of the machine considered in this study it is critical to clarify the interaction between the actual rotor current distribution and the MMF produced by each stator winding. The interaction, if any, between the currents in the two sets of stator windings must be studied as well. For this purpose a detailed, yet simple, dynamic model of the machine will be developed. The coupled magnetic circuit theory and complex space vector notation will be used through out the derivation. This technique is chosen because of its generality and the great deal of simplification that is achieved. The following general assumptions are made:

- negligible saturation,
- uniform airgap,

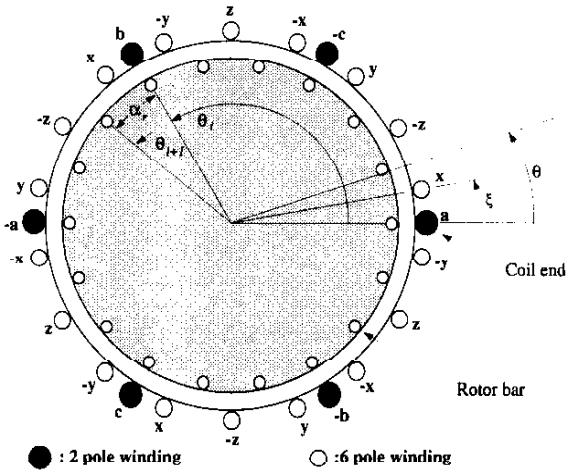

Fig. 4. Dual stator winding induction machine.

- stator windings sinusoidally distributed,
- no electrical interconnection between stators, *and*
- negligible inter-bar current

It is also assumed that the two stator windings are wound for 2 and 6 poles respectively and that one stator is displaced with respect to the other by a fix but arbitrary angle ξ. The main stator (2 pole) will be referred to as the *abc* windings and the secondary stator, having 6 poles, will be labeled as *xyz* windings. The rotor of the machine is a standard squirrel cage type. The proposed dual stator winding machine is schematically shown in Fig. 4.

A. Stator Flux

Since both stators are sinusoidally distributed in space but wound for a different number of poles (and electrically isolated) there is no mutual coupling due to main flux between them [9], [10]. However, since both windings share common slots and are in close proximity, there is a common leakage flux linking them. This gives rise to the so-called mutual leakage coupling [8], [11].

The total flux linked by the stator windings and due only to the stator currents $\mathbf{i}_{sabc}$ and $\mathbf{i}_{sxyz}$ can be written, in matrix form, as

$$\begin{bmatrix} \mathbf{\Lambda}_{ssabc} \\ \mathbf{\Lambda}_{ssxyz} \end{bmatrix} - \begin{bmatrix} \mathbf{L}_{s1} & \mathbf{L}_{s12} \\ \mathbf{L}_{s21} & \mathbf{L}_{s2} \end{bmatrix} \begin{bmatrix} \mathbf{i}_{sabc} \\ \mathbf{i}_{sxyz} \end{bmatrix} \tag{1}$$

where

$$\begin{bmatrix} \mathbf{\Lambda}_{ssabc} \\ \mathbf{\Lambda}_{ssxyz} \end{bmatrix} = \begin{bmatrix} \lambda_{ass} \\ \lambda_{bss} \\ \lambda_{css} \\ \lambda_{xss} \\ \lambda_{yss} \\ \lambda_{zss} \end{bmatrix}; \qquad \begin{bmatrix} \mathbf{i}_{sabc} \\ \mathbf{i}_{sxyz} \end{bmatrix} = \begin{bmatrix} i_{as} \\ i_{bs} \\ i_{cs} \\ i_{xs} \\ i_{ys} \\ i_{zs} \end{bmatrix} \tag{2}$$

$\mathbf{L}_{s1}$ and $\mathbf{L}_{s2}$ represent the self inductance matrices of the *abc* and *xyz* windings respectively. They are of the form: [9]

$$\mathbf{L}_{si} = \begin{bmatrix} L_{lsi} + L_{msi} & -\frac{L_{msi}}{2} & -\frac{L_{msi}}{2} \\ -\frac{L_{msi}}{2} & L_{lsi} + L_{msi} & -\frac{L_{msi}}{2} \\ -\frac{L_{msi}}{2} & -\frac{L_{msi}}{2} & L_{lsi} + L_{msi} \end{bmatrix} \tag{3}$$

The magnetizing inductance L_{msi} is known to be: [12]

$$L_{msi} = \frac{\pi \mu_o l r}{g} \left(\frac{N_{si}}{P} \right)^2 \tag{4}$$

where N_{si} is the total number of turns per phase of each winding set and P is the number of poles. L_{lsi} represents the total per-phase self leakage inductance of each winding and it can be calculated by traditional methods [14], [15].

The sub-matrices $\mathbf{L}_{s12}$ and $\mathbf{L}_{s21}$ account for the mutual leakage coupling between the two stator windings. In general, the leakage flux can be divided into slot, end winding, belt and zig-zag components and each one of them will contribute to the self and mutual leakage inductance. For simplicity, however, the mutual leakage due to the zig-zag and belt leakage components will be neglected and it will be assumed that they only contribute to the self leakage. Therefore, it will be assumed that only the slot and end winding components contribute to the mutual leakage. Furthermore it will be assumed that the end winding leakage varies as the slot leakage [8].

B. Slot Leakage Inductance

To study the mutual leakage term let us consider the winding distributions shown in Fig. 5. They correspond to a) fractional pitch due to the displacement ξ between stators, 60° phase belt, and b) fractional pitch, 30° phase belt. Note that, since the two set of windings have two and six poles respectively, their pitch angles α_1 and α_2 are in the ratio 6/2. In Fig. 5-a, defining p_1 and p_2 as the pitch of the *abc* and *xyz* windings respectively, for a variation of ξ between zero and 20° the corresponding pitch factors vary as $8/9 < p_1 < 1$ and $2/3 < p_2 < 1$.

As shown by Alger [15] and Lipo [16], the slot leakage can be divided into self leakage and mutual leakage. The self leakage represents that part of the flux produced by the in-phase current component (i.e., slots with coil sides belonging to the same phase). The mutual leakage accounts for the leakage flux due to having conductors from different phases sharing common slots. In general, for a two layer winding the self, (L_{sls}), and mutual, (L_{slm}), components of the slot leakage inductance can be expressed, as a function of the pitch p, by

$$L_{sls} = L_{lT} + L_{lB} + 2k_s(p)L_{lTB} \tag{5}$$

$$L_{slm} = k_m(p)L_{lTB} \tag{6}$$

where L_{lT} and L_{lB} are the slot leakage inductances associated to the coils in the top and bottom halves of the slots. They are calculated for the case of unity pitch and do not depend on winding pitch. The term L_{lTB} represents the mutual inductance between coils in the top and bottom halves of the slot. The quantities k_s and k_m are called slot factors and they correspond to proportionality constants that depend on the pitch.

For the winding distribution of Fig. 5-a, the phase belt slot leakage flux associated to phase *a*, when $8/9 < p_1 < 1$, is

$$\begin{aligned} \lambda_{sla} = (L_{lT1}+L_{lB1})i_{as} - L_{lTB1}k_{m1}(p_1)(i_{bs}+i_{cs}) \\ +2L_{lTB2}i_{xs} - (2 - k_{m2}(p_2))L_{lTB2}(i_{zs}+i_{ys}) \end{aligned} \tag{7}$$

The equations applying to the remaining phases of the *abc* winding can be found by symmetry and the corresponding

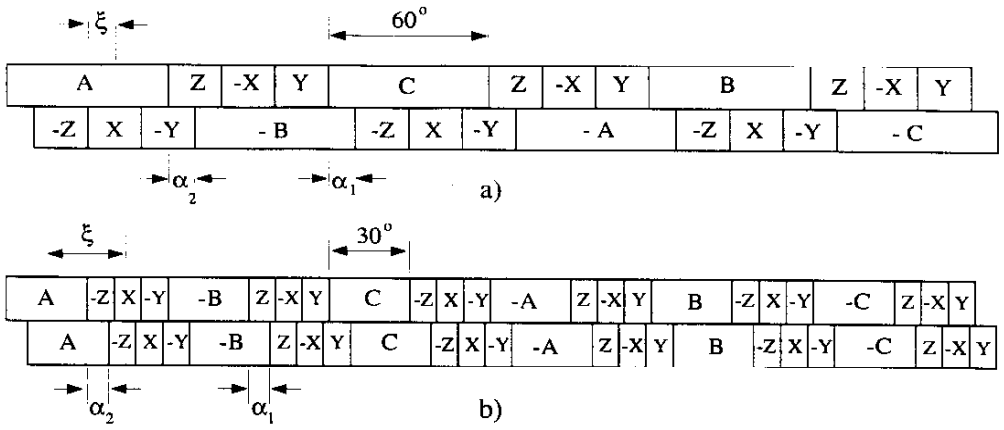

Fig. 5. Winding distribution for a) fractional pitch and variable displacement angle ξ, 60° phase belt, b) fractional pitch and variable displacement angle ξ, 30° phase belt.

slot leakage matrix inductance is

$$\mathbf{L}_{sl1} = \begin{bmatrix} L_{lT1}+L_{lB1} & -L_{lTB1}k_{m1} & -L_{lTB1}k_{m1} \\ -L_{lTB1}k_{m1} & L_{lT1}+L_{lB1} & -L_{lTB1}k_{m1} \\ -L_{lTB1}k_{m1} & -L_{lTB1}k_{m1} & L_{lT1}+L_{lB1} \end{bmatrix} + 2L_{lTB2}\begin{bmatrix} 1 & k_{m2}-2 & k_{m2}-2 \\ 1 & k_{m2}-2 & k_{m2}-2 \\ 1 & k_{m2}-2 & k_{m2}-2 \end{bmatrix} \tag{8}$$

A similar reasoning yields the slot leakage inductance matrix of the xyz winding

$$\mathbf{L}_{sl2} = -L_{lTB2}\begin{bmatrix} -1 & -1 & -1 \\ 1+k_{m2} & 1+k_{m2} & 1+k_{m2} \\ 1+k_{m2} & 1+k_{m2} & 1+k_{m2} \end{bmatrix} + \begin{bmatrix} L_{lT2}+L_{lB2} & 0 & 0 \\ 0 & L_{lT2}+L_{lB2} & -3k_{m2}L_{lTB2} \\ 0 & -3k_{m2}L_{lTB2} & L_{lT2}+L_{lB2} \end{bmatrix} \tag{9}$$

The slot factor k_{m1} must be zero when $p_1 = 1$ and one when $p_1 = 2/3$. Hence when $2/3 < p_1 < 1$

$$k_{m1} = 3 - 3p_1 \tag{10}$$

Similarly, k_{m2} must be zero when $p_2 = 1$ and one when $p_2 = 8/9$. Hence when $8/9 < p_2 < 1$

$$k_{m2} = 9 - 9p_2 \tag{11}$$

If the winding distribution of Fig. 5-b is considered instead, the results are similar and the structure of (8) and (9) remain unchanged [13].

Assuming that the end winding leakage behaves as the slot leakage, the mutual inductance matrix $\mathbf{L}_{s12}$ is proportional to the second term in (8). Clearly, the mutual inductance matrix $\mathbf{L}_{s21}$ will be proportional to the first term in (9).

Given the symmetric structure of the matrices $\mathbf{L}_{s12}$ and $\mathbf{L}_{s21}$ and assuming no neutral connection, it is apparent that after applying the space vector definition

$$\underline{\lambda}_{slabc} = \tfrac{2}{3}\left(\lambda_{sla} + \underline{a}\lambda_{slb} + \underline{a}^2\lambda_{slc}\right) \tag{12}$$

their contribution to the total flux vector will be zero.

This result is very important since it proves that both stator windings are fully decoupled and the total flux linked by the stator windings can be written as

$$\mathbf{\Lambda}_{sabc} = \mathbf{L}_{s1}\mathbf{i}_{sabc} + \mathbf{L}_{sr1}\mathbf{i}_r \tag{13}$$

for the primary winding and

$$\mathbf{\Lambda}_{sxyz} = \mathbf{L}_{s2}\mathbf{i}_{sxyz} + \mathbf{L}_{sr2}\mathbf{i}_r \tag{14}$$

for the secondary winding. The matrices $\mathbf{L}_{sr1}$ and $\mathbf{L}_{sr2}$ describe the mutual coupling between the stator and rotor circuits and they can be determined using winding functions [17]. As shown in [17], using complex vector representation, the stator flux associated to the *abc* winding can be written as

$$\underline{\lambda}_{sabc} = \left(L_{ls1} + \tfrac{3}{2}L_{ms1}\right)\underline{\mathbf{i}}_{s1} + \tfrac{2n\sin\delta}{\pi N_{s1}}L_{ms1}e^{j(\theta_r+\delta)}\underline{\mathbf{i}}_{r1} \tag{15}$$

where n is the number of rotor bars, δ is 1/2 the angle between rotor bars and the complex vector currents $\underline{\mathbf{i}}_{s1}$ and $\underline{\mathbf{i}}_{r1}$ are defined by

$$\underline{\mathbf{i}}_{s1} = \tfrac{2}{3}\left(i_{as} + \underline{a}i_{bs} + \underline{a}^2 i_{cs}\right) \tag{16}$$

$$\underline{\mathbf{i}}_{r1} = \tfrac{2}{n}\begin{bmatrix} 1 & \underline{b} & \underline{b}^2 & \cdots & \underline{b}^{n-1} \end{bmatrix}\begin{bmatrix} i_{r1} \\ i_{r2} \\ \vdots \\ i_{rn} \end{bmatrix} \tag{17}$$

with $\underline{a} = e^{j2\pi/3}$ and $\underline{b} = e^{j2\pi/n}$. The vector $[i_{r1}\ i_{r2}\cdots i_{rn}]^T$ represents the instantaneous rotor currents defined according to Fig. 6.

A similar analysis for the xyz winding yields [13]

$$\underline{\lambda}_{sxyz} = \left(L_{ls2} + \tfrac{3}{2}L_{ms2}\right)\underline{\mathbf{i}}_{s2} + \tfrac{2n\sin\frac{p}{2}\delta}{\pi N_{s2}}L_{ms2}e^{j\frac{p}{2}(\theta_r+\delta-\xi)}\underline{\mathbf{i}}_{r2} \tag{18}$$

where

$$\underline{\mathbf{i}}_{s2} = \tfrac{2}{3}\left(i_{xs} + \underline{a}i_{ys} + \underline{a}^2 i_{zs}\right) \tag{19}$$

and

$$\underline{\mathbf{i}}_{r2} = \tfrac{2}{n}\begin{bmatrix} 1 & \underline{b}^{\frac{p}{2}} & \underline{b}^{\frac{p}{2}2} & \cdots & \underline{b}^{\frac{p}{2}(n-1)} \end{bmatrix}\begin{bmatrix} i_{r1} \\ i_{r2} \\ \vdots \\ i_{rn} \end{bmatrix} \tag{20}$$

Note that because of the different number of poles considered in this case it is necessary to define a new rotor current space vector $\underline{\mathbf{i}}_{r2}$. The physical meaning of this new definition can be understood by recognizing that the equivalent electrical angle between adjacent rotor bars,

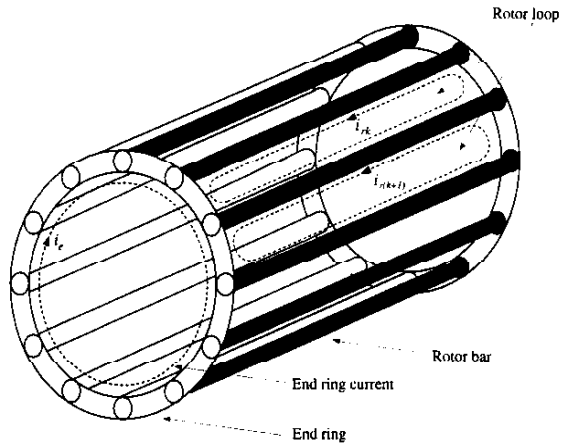

Fig. 6. Rotor current definition.

referred to the P pole xyz winding, is now $\frac{P}{2}\theta_r$ instead of θ_r. Also note that the actual rotor bar currents in (17) and (20) are the same.

Finally, the stator voltage equations for both stator windings are obtained by differentiating the flux linkages (15) and (18) and adding the resistive voltage drops. This procedure yields

$$\begin{aligned}\underline{\mathbf{v}}_{s1} &= r_{s1}\underline{\mathbf{i}}_{s1} + \left(L_{ls1} + \tfrac{3}{2}L_{ms1}\right)p\underline{\mathbf{i}}_{s1} \\ &\quad + \tfrac{2n\sin\delta}{\pi N_{s1}}L_{ms1}e^{j(\theta_r+\delta)}\left(p + j\omega_r\right)\underline{\mathbf{i}}_{r1}\end{aligned} \tag{21}$$

for the abc winding and

$$\begin{aligned}\underline{\mathbf{v}}_{s2} &= r_{s2}\underline{\mathbf{i}}_{s2} + \left(L_{ls2} + \tfrac{3}{2}L_{ms2}\right)p\underline{\mathbf{i}}_{s2} \\ &\quad + \tfrac{2n\sin\frac{P}{2}\delta}{\pi N_{s2}}L_{ms2}e^{j\frac{P}{2}(\theta_r+\delta-\xi)}\left(p + j\tfrac{P}{2}\omega_r\right)\underline{\mathbf{i}}_{r2}\end{aligned} \tag{22}$$

for the xyz winding. The complex vector voltages $\underline{\mathbf{v}}_{s1}$ and $\underline{\mathbf{v}}_{s2}$ are

$$\begin{aligned}\mathbf{v}_{s1} &= \tfrac{2}{3}\left(v_{as} + \underline{a}v_{bs} + \underline{a}^2 v_{cs}\right) \\ \underline{\mathbf{v}}_{s2} &= \tfrac{2}{3}\left(v_{xs} + \underline{a}v_{ys} + \underline{a}^2 v_{zs}\right)\end{aligned} \tag{23}$$

It is important to notice that the stator current $\underline{\mathbf{i}}_{s1}$ depends only on the applied voltage $\underline{\mathbf{v}}_{s1}$ and the rotor current $\underline{\mathbf{i}}_{r1}$. Similarly the current $\underline{\mathbf{i}}_{s2}$ depends only on the applied voltage $\underline{\mathbf{v}}_{s2}$ and the rotor current $\underline{\mathbf{i}}_{r2}$. This result verifies the known fact that, for a sinusoidally distributed winding, there only exists coupling between current distributions of the same number of poles.

C. Rotor Flux

The rotor flux can be divided into three components, one due to the rotor currents $\mathbf{i}_r$ and two due to the stator currents $\mathbf{i}_{sabc}$ and $\mathbf{i}_{sxyz}$. In matrix form

$$\begin{bmatrix}\lambda_{r1}\\ \lambda_{r2}\\ \vdots\\ \lambda_{rn}\end{bmatrix} = \mathbf{L}_r\begin{bmatrix}i_{r1}\\ i_{r2}\\ \vdots\\ i_{rn}\end{bmatrix} + \mathbf{L}_{rs1}\begin{bmatrix}i_{as}\\ i_{bs}\\ i_{cs}\end{bmatrix} + \mathbf{L}_{rs2}\begin{bmatrix}i_{xs}\\ i_{ys}\\ i_{zs}\end{bmatrix} \tag{24}$$

In general, the complex vector representation of the rotor flux is defined by the vector transformation

$$\underline{\boldsymbol{\lambda}}_r = \tfrac{2}{n}\begin{bmatrix}1 & \underline{b}^{\frac{P}{2}} & \underline{b}^{\frac{P}{2}2} & \cdots & \underline{b}^{\frac{P}{2}(n-1)}\end{bmatrix}\begin{bmatrix}\lambda_{r1}\\ \lambda_{r2}\\ \vdots\\ \lambda_{rn}\end{bmatrix} \tag{25}$$

where P is given by the number of poles of the stator winding. Setting $P = 2$ in (25) and applying it to (24) yields the rotor flux referred to the 2 pole stator winding.

It is clear that the first two terms of (24) correspond to those of the single stator machine and they are given by [17]

$$\underline{\boldsymbol{\lambda}}_{rr} = \underbrace{\left(2L_b(1-\cos\alpha_r) + 2L_e + \tfrac{\mu_o l r}{g}\alpha_r\right)}_{L_{r1}}\underline{\mathbf{i}}_{r1} \tag{26}$$

and

$$\underline{\boldsymbol{\lambda}}_{rs1} = \tfrac{6\sin\delta}{\pi N_{s1}}L_{ms1}e^{-j(\theta_r+\delta)}\underline{\mathbf{i}}_{s1} \tag{27}$$

where L_b and L_e represent the bar and end-ring segment inductance respectively and g is the airgap length.

The last term of (24) represents the contribution due to the secondary stator winding currents. Following the same technique, it can be shown that

$$\begin{aligned}\underline{\boldsymbol{\lambda}}_{rs2} = \tfrac{2\sin\frac{P}{2}\delta}{\pi N_{s2}}L_{ms2}\Big\{&e^{j\frac{P}{2}(\theta_r+\delta-\xi)}\,\underline{\mathbf{i}}^*_{s2}\textstyle\sum_{i=0}^{n-1}\underline{b}^{(\frac{P}{2}+1)i} \\ &+e^{-j\frac{P}{2}(\theta_r+\delta-\xi)}\underline{\mathbf{i}}_{s2}\textstyle\sum_{i=0}^{n-1}\underline{b}^{-(\frac{P}{2}-1)i}\Big\}\end{aligned} \tag{28}$$

However, for $P > 2$, both summations in (28) are identically zero, hence $\underline{\boldsymbol{\lambda}}_{rs2}$ is identically zero, regardless of the value of $\underline{\mathbf{i}}_{s2}$, and the total rotor flux, in the 2 pole winding subspace, corresponds to the sum of (26) and (27).

Finally, taking the time derivative of the rotor flux vector and adding the resistive voltage drop gives the rotor voltage equation in the subspace defined by the 2 pole winding. This yields

$$\begin{aligned}\underline{\mathbf{0}} &= r_{r1}\underline{\mathbf{i}}_{r1} + L_{r1}p\underline{\mathbf{i}}_{r1} \\ &\quad + \tfrac{6\sin\delta}{\pi N_{s1}}L_{ms1}e^{-j(\theta_r+\delta)}\left(p - j\omega_r\right)\underline{\mathbf{i}}_{s1}\end{aligned} \tag{29}$$

with $r_{r1} = 2R_e + 2R_b\left(1-\cos\alpha_r\right)$.

A similar analysis for the P pole winding reveals that, in this case, the contribution of the second term in (24) is zero and the rotor voltage equation in the subspace defined by the P pole winding is

$$\begin{aligned}\underline{\mathbf{0}} &= r_{r2}\underline{\mathbf{i}}_{r2} + L_{r2}p\underline{\mathbf{i}}_{r2} \\ &\quad + \tfrac{6\sin\frac{P}{2}\delta}{\pi N_{s2}}L_{ms2}e^{-j\frac{P}{2}(\theta_r+\delta-\xi)}\left(p - j\omega_r\right)\underline{\mathbf{i}}_{s2}\end{aligned} \tag{30}$$

where r_{r2} represents the equivalent rotor resistance and L_{r2} is the equivalent rotor inductance in the P pole subspace, yielding

$$r_{r2} = 2R_e + 2R_b\left[1-\cos\left(\tfrac{P}{2}\alpha_r\right)\right] \tag{31}$$

and

$$L_{r2} = 2L_b\left[1-\cos\left(\tfrac{P}{2}\alpha_r\right)\right] + 2L_e + \tfrac{\mu_o l r}{g}\left(\tfrac{P}{2}\alpha_r\right) \tag{32}$$

Note that although the instantaneous rotor current distribution simultaneously contain two components of different frequencies and pole number, each stator field is capable of interacting only with that part of the rotor field with the "correct" number of poles. This is true

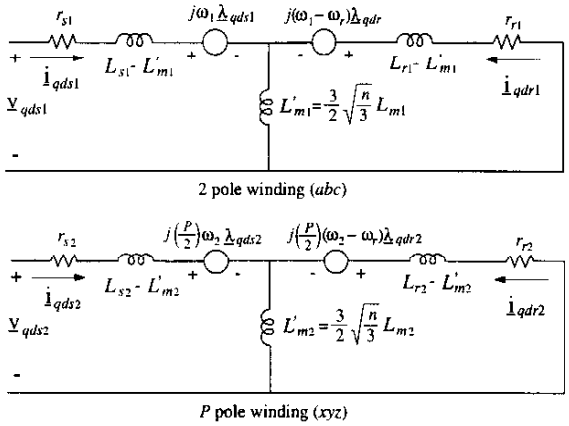

Fig. 7. Complex vector model of the dual stator winding squirrel cage induction machine.

not only in an average basis but also instantaneously. It is well known that sinusoidally distributed windings only couple with fields wound for the same number of poles, however the rotor cage is clearly not a sinusoidal winding and one might expect that the presence of two superimposed flux distributions would give rise to pulsating torques. However, this is not the case for the proposed dual stator winding machine. An equivalent circuit, using d–q notation, is shown in Fig. 7

Neglecting saturation, the electromagnetic torque can be expressed as the partial variation of the co-energy with respect to position [9]

$$T_e = \left[\mathbf{i}_{sabc}^T \; \mathbf{i}_{sxyz}^T\right] \frac{\partial}{\partial \theta_r} \begin{bmatrix} \mathbf{L}_{sr1} \\ \mathbf{L}_{sr2} \end{bmatrix} \mathbf{i}_r \tag{33}$$

which can be written as the separate sum of the torques produced by each set of stator currents

$$T_e = \mathbf{i}_{sabc}^T \frac{\partial \mathbf{L}_{sr1}}{\partial \theta_r} \mathbf{i}_r + \mathbf{i}_{sxyz}^T \frac{\partial \mathbf{L}_{sr2}}{\partial \theta_r} \mathbf{i}_r \tag{34}$$

Substituting the corresponding matrices and carrying out the differentiation yields

$$T_e = -\left(\frac{3n \sin\delta}{\pi N_{s1}}\right) L_{ms1} Im\Big\{ e^{j(\theta_r+\delta)} \underline{\mathbf{i}}_{s1}^* \underline{\mathbf{i}}_{r1} + e^{j3(\theta_r+\delta-\xi)} \frac{N_{s2} \sin(3\delta)}{3N_{s1} \sin\delta} \underline{\mathbf{i}}_{s2}^* \underline{\mathbf{i}}_{r2} \Big\} \tag{35}$$

where we have used $P = 6$. Since $\underline{\mathbf{i}}_{r1}$ and $\underline{\mathbf{i}}_{r2}$ are orthogonal vectors the two torque components can be controlled independently by the stator currents.

IV. Torque and Speed Control

Since the proposed machine behaves as two independent induction machines, mechanically coupled through the shaft, all the known control techniques used in induction machine drives are also applicable to the dual stator winding machine.

In general there are two distinct modes of operation, the low speed (i.e., frequencies below a few hertz) and the medium to high speed range. In the low speed range the goal is to maintain the frequency of the 2 pole winding above a minimum level (about 3 Hz) and the torque is

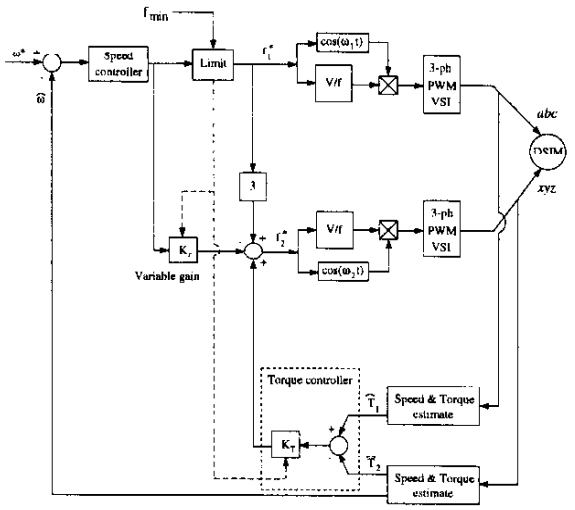

Fig. 8. Proposed control scheme for constant V/f operation.

controlled by adjusting the frequency of the 6 pole winding. By keeping the frequency above this pre-set limit the influence of the stator resistance is minimized, hence simplifying the control. In this mode the two MMF's rotate asynchronously but because of the reduced frequency the additional losses caused by saturation should be minimal.

In the medium to high speed range the negative effect of the stator resistance is not a concern and the frequencies are kept in the ratio 1:3. This constraint guarantees a nearly trapezoidal flux distribution and the torque is controlled by adjusting the magnitude of the applied voltages. The trapezoidal shape, in turn, allows for slightly greater two pole flux than when only the two pole winding is excited thereby producing slightly more torque per ampere.

A. Constant V/f Control

The operation and control will be explained with the help of Fig. 3. As shown in this figure there are two different operating modes. For high speed both stators are fed with voltages of the same frequency. This produces the torque-speed curves of Fig. 3-a. The output torque for a given rotor speed corresponds to the algebraic sum of the torques T_1 and T_2 produced by each of the stator. The torque produced by each winding is controlled by adjusting the magnitude of the stator voltages.

When both stators are fed with different frequencies the result is that shown in Fig. 3-b. By fixing the frequency of one of the stators, say *abc*, the total output torque can be adjusted by controlling the frequency (and voltage) supplied to the *xyz* winding f_2. In the case shown in Fig. 3-b an increase in torque requires an increase in f_2 and vice versa. In this case one of the stator windings (*abc*) operates in the motoring region while the other (*xyz*) operates as a generator. Note that this operating mode corresponds to the one required to operate at zero speed and that the torque can be controlled from zero to rated value. A simplified block diagram of the proposed control scheme is shown in Fig. 8.

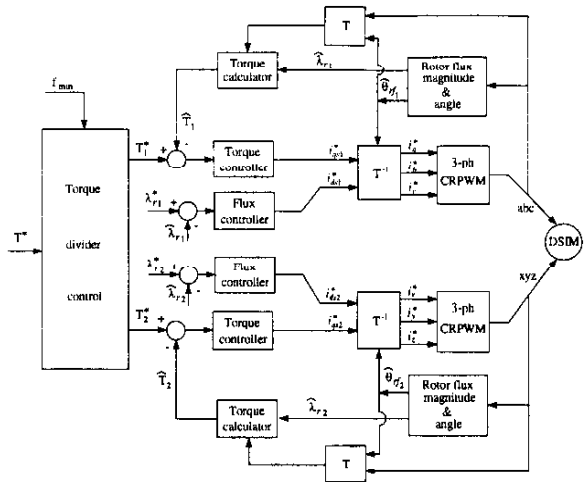

Fig. 9. Proposed control scheme for field oriented operation.

B. Vector Control

A simplified block diagram of the proposed control scheme is given in Fig. 9. As in the constant V/f method the vector control is divided into two operating regions: a high speed range defined by frequencies above a minimum frequency f_{min} and a low speed range for frequencies below f_{min}. For the high speed region the proposed control method is quite straight forward dividing the output torque among the two windings as to yield similar stator currents and a nearly trapezoidal flux distribution. In the low speed range a negative torque command is given to the secondary winding hence increasing the torque produced by the primary winding which yields an increased stator frequency. The goal is to maintain the primary stator frequency at a constant value equal to f_{min}.

V. Simulation Results

To prove the correctness of the complex space vector model of the dual stator machine a complete set of simulations has been carried out. The results from the space vector model are compared to those obtained from a full matrix model of the machine. Fig. 10 shows both set of results superimposed. It is clear that both simulations are identical hence proving the validity of the complex vector model. As shown in Fig. 10 the rotor currents contain two different frequencies dictated by the frequency of each of the stator currents and the rotor mechanical speed. Although the rotor currents simultaneously produce two field distributions that rotate at different speeds, because of the different number of poles and the sinusoidal characteristic of the stator windings, they do not give rise to harmonic torques.

Simulation results using the control techniques proposed in the previous section are shown in figures 11 and 12, hence proving the feasibility of the method.

VI. Experimental Results

A 5 Hp prototype is currently under construction and the experimental results will be reported shortly.

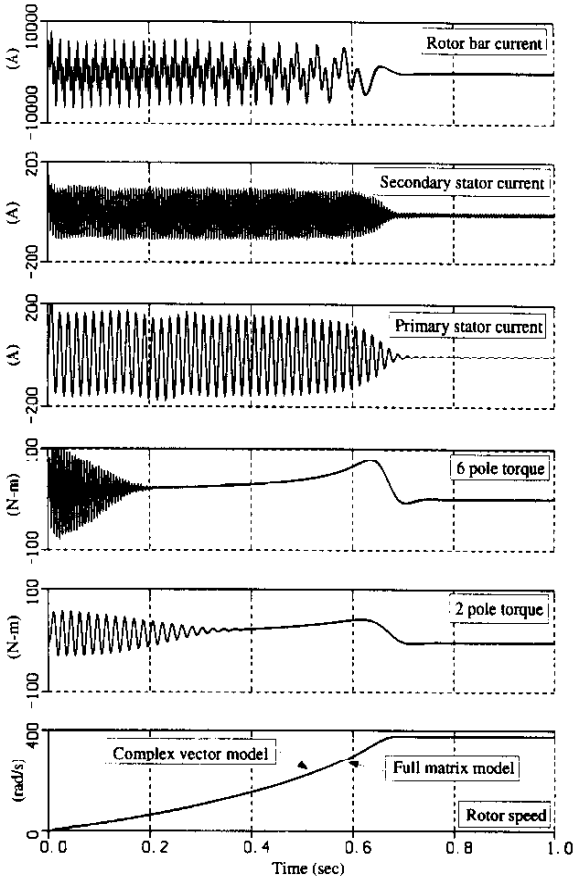

Fig. 10. Full matrix and complex vector model simulation results for a free acceleration run at 60 Hz (f_2 = 180 Hz). Complex vector and full matrix model traces are superimposed.

VII. Conclusions

A new type of dual stator winding induction machine has been presented. The most relevant characteristic of the new machine is that the two stator windings are wound for a dissimilar number of poles. This feature yields two independent torques that can be controlled as desired to produce the net output torque. In addition, the problem of high circulating harmonic currents common to dual stator induction drives is also eliminated. The machine is especially well suited for both constant V/f and sensorless FO control.

By implementing an adequate torque control scheme it is possible to operate at stand still and, at the same time, limit the minimum frequency at which the 2 pole stator winding operates. This is an important feature since it reduces the impact of the stator resistance voltage drop at low frequencies and greatly simplifies the implementation of sensorless control algorithms.

REFERENCES

[1] P. L. Alger, E. H. Freiburghouse and D. D. Chase, *"Double windings for turbine alternators"*, AIEE Transactions, Vol. 49, January 1930, pp. 226-244.

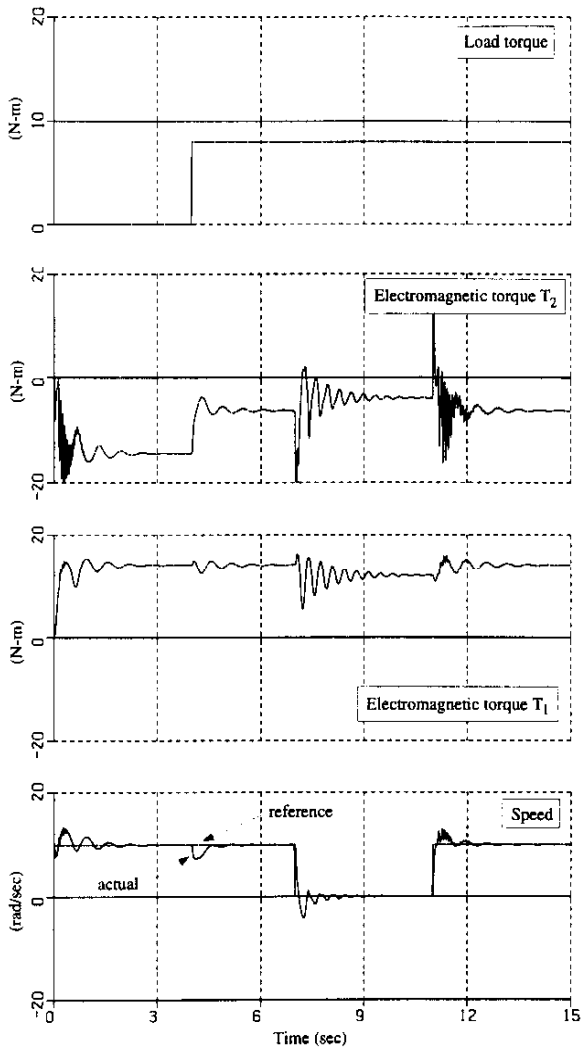

Fig. 11. Constant V/f operation at stand still.

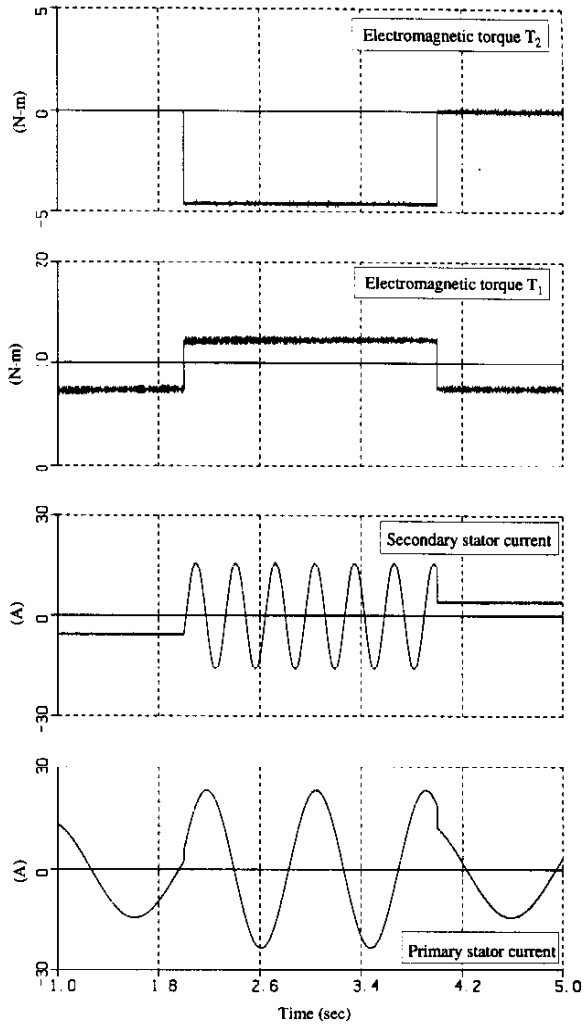

Fig. 12. Direct field orientation at stand still.

[2] P. W. Franklin, *"A theoretical study of the three phase salient pole type generator with simultaneous AC and bridge rectified DC output"*, IEEE Transactions on Power App. and Systems, Vol. PAS-92, No. 2, March/April 1973, pp. 543-557.

[3] T. Kataoka, E. H. Watanabe and J. Kitano, *"Dynamic control of a current-source inverter/double-wound synchronous machine system for AC power supply"*, IEEE Transactions on Industry Applications, Vol. IA-17, No. 3, May/June 1981, pp. 314-320.

[4] J. R. Fu and T. A. Lipo, *"Disturbance free operation of a multiphase current regulated motor drive with an opened phase"*, IEEE Transactions on Industry Applications, Vol. 30, No. 5, September/October 1994, pp. 1267-1274.

[5] J. C. Salmon and B. W. Williams, *"A split-wound induction motor design to improve the reliability of PWM inverter drives"*, IEEE Transactions on Industry Applications, Vol. IA-26, No. 1, January/February 1990, pp. 143-150.

[6] E. F. Fuchs and L. T. Rosenberg, *"Analysis of an alternator with two displaced stator windings"*, IEEE Transactions on Power App. and Systems, Vol. PAS-93, No. 6, November/December 1974, pp. 1776-1786.

[7] K. Gopakumar, V. T. Ranganathan and S. R. Bhat, *"Split-phase induction motor operation from PWM voltage source inverter"*, IEEE Transactions on Industry Applications, Vol. 29, No. 5, September/October 1993, pp. 927-932.

[8] T. A. Lipo, *"A d-q model for six phase induction machines"*, International Conference on Electric Machines, Athens, Greece, 1980, pp. 860-867.

[9] D. W. Novotny and T. A. Lipo, *Vector Control and Dynamics of AC Drives*, Clarendon Press-Oxford, 1996.

[10] S. A. Nasar, *"Electromechanical energy conversion in nm-winding double cylindrical structures in presence of space harmonics"*, IEEE Transactions on Power App. and Systems, Vol. PAS-87, No. 4, April 1968, pp. 1099-1106.

[11] R. Schiferl, *"Detailed analysis of a six phase synchronous machine with AC and DC stator connections"*, Ph.D. Dissertation, Purdue University, West Lafayette, Indiana, 1982.

[12] G. R. Slemon, *Electric Machines and Drives*, Addison-Wesley Publishing Co., 1992.

[13] A. Muñoz-García, *"Analysis and control of a dual stator winding squirrel cage induction machine for high performance drives"*, Preliminary Ph.D. Thesis proposal, University of Wisconsin-Madison, 1997.

[14] A. S. Langsdorf, *Theory of Alternating Current Machinery*, Second Edition, McGraw-Hill, 1955.

[15] P. L. Alger, *Induction Machines*, Gordon and Breach Science Publishers, Second Edition, 1970.

[16] T. A. Lipo, *Introduction to AC Machine Design*, University of Wisconsin-WisPERC, 1996.

[17] A. Muñoz-García and T. A. Lipo, *"Complex vector model of the squirrel cage induction machine including instantaneous rotor bar currents"*, IEEE Industry Applications Society 1998 Annual Meeting, St. Louis Missouri, 1998, in press.